

Cite this: *RSC Sustainability*, 2025, 3, 5241

# Sustainable eco-friendly scale-up synthesis of polytartaric acid using renewable feedstocks

Iulia Rigo,<sup>a</sup> Alexander Bunge,<sup>b</sup> Lucian-Cristian Pop,<sup>a</sup> Natalia Terenti<sup>ib</sup>\*<sup>b</sup> and Alexandrina Nan<sup>ib</sup>\*<sup>b</sup>

Scaling up polymerization reactions presents significant challenges due to unpredictabilities in the entire process, requiring careful attention to both mass and heat transfer dynamics. This work reveals the scale-up of the self-catalyzed polyesterification of tartaric acid from 5 g to 500 g (a scale-up factor of 100) through a simplified method without using a catalyst or solvent. In this instance, key operating parameters—including reaction conditions such as temperature, duration, and chemical composition—are kept constant, thus standardizing the reaction conditions. A pilot plant designed to simulate potential industrial sizes has been established to optimize the implementation of larger scales. The primary focus of the scale-up process is maintaining a consistent heat removal capacity across different reactor sizes. Additionally, the impact of upscaling on the polymer structure is analysed using solid-state <sup>13</sup>C-NMR and Fourier Transform Infrared spectroscopy (FTIR), which provide measurable criteria for the success of the procedure. Finally, this paper examines the changes in the thermal conductivity properties of polytartaric acid resulting from the polymerisation scale-up process.

Received 14th August 2025  
Accepted 14th September 2025

DOI: 10.1039/d5su00667h

rsc.li/rscsus

## Sustainability spotlight

This study enhances the sustainable production of carboxylic polymers by scaling up the catalyst- and solvent-free polyesterification process utilizing tartaric acid. Our research outlines a more efficient and environmentally benign pathway for synthesizing biopolymers at an industrial scale. Utilizing tartaric acid derived from wine industry waste underscores a circular economy approach, effectively converting agricultural by-products into high-value materials. This methodology not only mitigates environmental impacts but also demonstrates a successful application of green chemistry principles coupled with waste valorization in scalable manufacturing contexts. Furthermore, our work directly contributes to the advancement of Sustainable Development Goals (SDGs), specifically SDG 12 (Responsible Consumption and Production) and SDG 13 (Climate Action). Our methodology aligns with the principles of the circular economy by prioritizing renewable feedstocks and ensuring biodegradability at the end of life. We assert that scientific innovation is pivotal in fostering a sustainable future, and we are dedicated to delivering practical, scalable solutions that reflect this commitment.

## Introduction

The unprecedented industrial revolution that follows the doctrine of circular economy will bring about a swift escalation in the availability of innovative, inexpensive, and biodegradable materials with customisable features. Polymers are among the materials found in nearly every component surrounding us. Natural polymers, such as cellulose and rubber, have been utilised for centuries, followed by the invention of the first synthetic polymer, Bakelite, a phenol-formaldehyde derivative, in 1907. Over the past century, significant advancements in polymer science have occurred, resulting in global commercial plastic production exceeding 413.8 million metric tons in 2023,

driven by the extensive demand for polymeric products. Synthetic polymers have replaced conventional materials like wood, metal, and glass due to their flexibility, strength, and practicality, while the latter are frequently heavy, challenging to manipulate, costly, and cumbersome.<sup>1,2</sup> These specifications for polymers and composites have posed numerous hurdles for researchers in materials science, including the synthesis of novel polymeric compounds and the subsequent scaling of the material for future industrial uses. Generally, progressing from a newly developed compound at the laboratory scale to an industrial scale necessitates supplementary intermediate steps. The process involves achieving an ideal equilibrium among chemistry, properties, compliance, and economic considerations, frequently requiring interdisciplinary collaboration. Unfortunately, the overabundant disposal of non-degradable plastic waste in landfills results in significant environmental repercussions, as the accumulated debris can persist in ecosystems for centuries.<sup>3-7</sup> Consequently, extensive research has focused on identifying degradable alternatives that can be

<sup>a</sup>Babeş-Bolyai University, Faculty of Chemistry and Chemical Engineering, 11 Arany János Str., Cluj-Napoca, 400028, Romania

<sup>b</sup>National Institute for Research and Development of Isotopic and Molecular Technologies, 67-103 Donat Str., 400293, Cluj-Napoca, Romania. E-mail: alexandrina.nan@itim-cj.ro



used as commercial thermoplastics for single-use applications. Among the degradable polymers derived from this research, aliphatic polyesters exhibit remarkable potential due to their origin from renewable resources. Their degradation products, whether chemical or enzymatic, are environmentally benign and recyclable.<sup>8–13</sup>

Scaling up polymerisation reactions is a critical process in the chemical industry, enabling the transition from laboratory-scale experiments to large-scale industrial production, providing furnishing applications, including plastics, in medicine, electronics, coatings, adhesives, tissue engineering, sensors, and other fields.<sup>14–19</sup> The scale-up process presents several challenges, primarily due to the significant changes in reaction conditions, such as temperature and heat transfer, pressure, and mixing, that occur when transitioning from a small-scale setup to a larger one. Moreover, maintaining consistent mixing and ensuring uniform distribution of reactants are crucial for achieving the desired polymer properties. Additionally, careful consideration of reaction kinetics, thermodynamics, and hydrodynamics is required to ensure that the final product meets the necessary specifications. Overall, the successful scale-up of polymerisation reactions involves a thorough understanding of the underlying chemical processes and the implementation of advanced analytical techniques and process control strategies to optimise the reaction conditions and ensure product quality.<sup>20–26</sup>

Aliphatic polyesters represent a significant class of materials with considerable potential for applications in various sectors, including environmental, biomedical, agricultural, and pharmaceutical fields. They are regarded as one of the most promising categories of biodegradable polymers, offering significant environmental advantages. The selection of the appropriate monomer is critical as it directly influences the properties of the final product. Tartaric acid (TA), a naturally occurring organic compound abundantly found in wine production by-products (grape marc and lees), has become an intriguing feedstock for polymer synthesis. By converting wine waste into functional biopolymers, researchers are paving the way for a more environmentally friendly alternative to traditional plastic materials.<sup>27–30</sup> L-Tartaric acid has been utilized in the synthesis of polyamides, poly(ester amides), and polycarbonates. Additionally, tartaric acid-based polyesters have been synthesized. However, these polyesters tend to have low molecular weights and are mostly insoluble due to the participation of pendant hydroxyl groups in the polycondensation process, which results in crosslinked polymers.<sup>31–43</sup>

In this study, we will outline our progression from the synthesis of poly(tartaric acid) (PTA) to optimisation and scaling, adhering to the three fundamental concepts of our research: sustainability, circular economy, and green chemistry. PTA is a recent polymer synthesised by our group from a biologically derived precursor, tartaric acid, by a straightforward thermal treatment that does not require solvents or catalysts.<sup>44</sup> The presence of multiple carboxy groups (–COOH) within the polymer chain enhances the versatility of the synthesised polymer, enabling a diverse array of applications. These include cosmetics, biomedicine, agriculture, and superplasticisers, which serve as high-range water reducers in the formulation of

high-strength concrete and self-compacting concrete. This article discusses the scaling of the polymerization reaction of tartaric acid TA to PTA, focusing on essential concepts, critical parameters, and potential challenges encountered during the transition from small-scale laboratory research to large-scale manufacturing. This exploration aims to elucidate the novel methodologies and collaborative initiatives propelling the future of PTA synthesis, facilitating its extensive adoption and utilisation. PTA can become a significant component in biodegradable packaging, the textile industry, agriculture, cosmetics, and personal care products. Our motivation for selecting tartaric acid in our research stems from its widespread availability as a by-product in the wine industry, particularly in wine waste. It is important to consider the environmental impacts associated with extracting and converting waste into tartaric acid, encouraging sustainable practices throughout.

## Results and discussion

The scale-up process remains a significant challenge in the field of chemical engineering. It establishes a connection between breakthroughs formulated in laboratory settings and practical inventions that operate efficiently in industry contexts. Enhancing a process often reveals challenges that are not apparent at a smaller scale. Thus, constructing a pilot plant is crucial before launching a new product into production. Nonetheless, owing to the numerous aspects that can affect product properties and process advancement, a universal formula for the scale-up procedure does not exist. Success often depends on expertise, innovative concepts, and a willingness to learn from mistakes, which may ultimately yield the desired results. Scaling up the polymerization reaction of tartaric acid necessitates careful consideration of a critical factor: temperature. This consideration is crucial for facilitating a seamless



Scheme 1 Synthesis of PTA.



transition from a laboratory to an industrial scale while maintaining efficiency and reproducibility (Scheme 1).

### Scale up of the polymerization PTA reaction

Several small-scale reactions were first performed to validate the feasibility of scaling up the **PTA** synthesis reaction, ensuring that the polymerisation process was consistent and reproducible. These preliminary experiments provided crucial insights into the reaction kinetics, product yield, and temperature conditions, laying the groundwork for subsequent scale-up efforts (Table 1).

To optimise the production costs of **PTA**, we have implemented a strategy to investigate the polymerisation of tartaric acid at various temperature ranges. We aim to develop a more energy-efficient polymerisation process by lowering the reaction temperature. As shown in Table 1, we synthesised samples **PTA 3** at 150 °C and **PTA 4** at 140 °C. The yields of these two polymeric samples, synthesised at lower temperatures, were higher than those of the samples synthesised at higher temperatures. This indicates that not all the tartaric acid monomers polymerize entirely at the lower temperatures, resulting in a higher yield. The increased yield may be due to the incomplete elimination of intermolecular water and carbon dioxide in the cases of **PTA 3** and **PTA 4**, which can enhance the overall yield. However, after titration of the carboxy groups and FTIR analysis of the FTIR spectra, we determined that the optimal polymerisation temperature for tartaric acid is 160 °C. This finding supports the argument for the best conditions for the polymerisation reaction.

**PTA** chains are defined by the presence of multiple carboxy (–COOH) functional groups, which significantly influence their chemical properties and reactivity. To assess the impact of temperature and the scaling-up process on these groups, we conducted a quantification through titration (refer to Table 1, last two columns). We selected bromothymol blue as the indicator for this analysis due to its specific pH transition range. During the titration process, this indicator helps pinpoint the equivalence point by a sharp change in the pH of the solution. At the equivalence point, the moles of acid and base are equal, resulting in a neutral solution. The titration procedure is based on the neutralization reactions between the –COOH groups of **PTA** and a strong base, such as sodium hydroxide (NaOH). This method allows for the precise measurement of the acidic functional groups present in the sample. The volume of NaOH

solution used was recorded and is presented in Table 1 (penultimate column). From these values, we calculated the millimoles per gram ( $\text{mmol g}^{-1}$ ) of carboxy groups in the polymer chain (last column of Table 1). This measurement enables us to determine the quantity of carboxy (COOH) groups in the polymer chain. The titration was conducted promptly because the presence of NaOH can trigger a depolymerization reaction in the **PTA** through the hydrolysis of ester moieties. This reaction may increase the number of carboxylic groups, potentially introducing errors into the results. Despite the uncertainties that may arise from polymer fragmentation under basic conditions, we observed that in the case of polymers synthesized at lower temperatures (150 °C and 140 °C), the number of  $\text{mmol g}^{-1}$  of carboxy groups is lower compared to those produced at higher temperatures.

Scaling up polymerization synthesis for **TA** presents a unique set of challenges. To maintain molecular integrity and yield consistency, precise control over reaction parameters, namely temperature, particle size of **TA**, and time, is required. The transition from laboratory-scale synthesis to industrial production necessitates adjustments in reactor design to maintain thermal stability and heat transfer, optimise reaction kinetics, and minimise side-product formation.

Fig. 1 illustrates a scaled-up installation for the polymerization reaction of tartaric acid. The reactor features a double-jacket construction made of steel and is classified as a Continuous Stirred-Tank Reactor (CSTR). Thus, the experimental procedure is designed to be conducted in a jacketed batch reactor equipped with an internal stirrer and a temperature control valve, ensuring uniform mixing and precise thermal regulation throughout the process. Initially, tartaric acid was ground into a fine powder using Grinder 2 to increase its surface area and enhance its



Fig. 1 Schematic representation of the experimental setup for scaling up the polymerization reaction.

Table 1 Description of samples produced to scale up the synthesis of polytartaric acid

Sample	TA [g]	Temp. [°C]	PTA [g]	Yield [%]	NaOH 0.1 M for neutralization [g]	Carboxy groups in PTA [ $\text{mmol g}^{-1}$ ]
PTA 1	5	160	3.95	79	14.93	7.32
PTA 2	5	160	3.85	77	15.9	7.25
PTA 3	5	150	4.13	82.6	10.74	5.75
PTA 4	5	140	4.66	93.2	7.45	3.62
PTA 5	5	160	3.85	77	12.31	7.19
PTA 6	5	160	4.02	80.4	11.15	6.03
PTA 7	10	160	7.71	77.1	17.99	8.17
PTA 8	50	160	40.12	80.2	16.52	7.83
PTA 9	500	160	356.85	71.37	12.99	6.50



reactivity. The finely milled tartaric acid was then carefully introduced into the reactor vessel. Once the reactant was loaded, the reactor was closed, and the agitation system was activated to promote homogeneous mixing. The temperature was gradually raised and maintained at 160 °C, while the reaction mixture was continuously stirred for a period of six hours.

At the end of the reaction time, a solid product with a distinct brown colouration was observed, indicating that the intended reaction had successfully progressed. The solid material was then discharged from the reactor and subjected to a secondary grinding process using Mill 4. This final milling step was performed to achieve a uniform particle size distribution, which is suitable for further analysis or downstream processing. The final polymerized **PTA** exits the system, ready for subsequent applications.

### Solid state $^{13}\text{C}$ -NMR

The  $^{13}\text{C}$  solid-state NMR spectrum of polytartaric acid exhibits distinct peaks, providing insight into its molecular structure (Fig. 2). The peaks around 170 ppm likely correspond to the carboxy and ester groups present in the polytartaric acid structure. The signals around 75 ppm may arise from hydroxy-bearing carbons, such as those adjacent to oxygen functionalities within the polymer backbone. In the cases of **PTA 1**, **PTA 8**, and **PTA 9**, the NMR signals keep the same shape, indicating that the upscaling reaction does not have any influence on the structure of the polymers, nor does it result in the elimination of more carbon dioxide during the reaction or the remaining of unreacted tartaric acid.

In the case of the sample **PTA 3**, the signal observed at 170 ppm begins to show signs of splitting, indicating that some of the tartaric acid remains unreacted. This splitting suggests that the carbon atoms in the carboxy group generate a stronger signal, separating the carbon signal associated with the carboxy group from that of the ester group.



Fig. 2  $^{13}\text{C}$  ss-NMR spectra of **PTA 1** (purple), **PTA 8** (green line), **PTA 9** (red line) and **PTA 3** (dark-blue line) recorded at 14 kHz spinning frequency.

### FTIR spectroscopy

FTIR spectroscopy is a valuable tool for analyzing the structural and chemical properties of **PTA**. The FTIR spectra depicted in Fig. S1 illustrate the characteristic functional groups present in **PTA** samples synthesized before scaling up the polymerization reaction. Significant adsorption bands in the spectra indicate the successful polymerization of tartaric acid and the formation of **PTA**. Fig. 3 illustrates the spectral profiles of the samples involved in the scale-up reaction. These spectra offer detailed insights into the composition and characteristics of the **PTA** samples, providing a basis for evaluating the reaction's progression and reproducibility during the scaling-up process. When the reaction is scaled up, the FTIR spectra reveal that the adsorption bands of key functional groups, such as carboxylic and hydroxy groups, do not undergo significant changes. This consistency in the spectral features indicates that the molecular structure and chemical integrity of **PTA** are maintained during the up-scaling process. The broad absorption bands around 3100–3500  $\text{cm}^{-1}$  correspond to the stretching vibrations of hydroxy groups. A weak doublet appears at 2868 and 2933  $\text{cm}^{-1}$  due to the stretching of the C–H bonds. The strong, broad absorption bands around 1750  $\text{cm}^{-1}$  indicate the stretching vibration of the carbonyl group ( $-\text{C}=\text{O}$ ), highlighting the presence of both carboxy and ester groups. A broad shoulder follows this region at 1635  $\text{cm}^{-1}$ , which indicates an absorption band of particular interest. This band is associated with the bending mode of the hydroxy groups in the polymer chain<sup>45</sup> but also corresponds to the adsorption band of carboxylate ions. Moreover, the absorption bands between 1200–1300  $\text{cm}^{-1}$  represent C–O–C stretching vibrations, suggesting ester linkages formed during the polymerization process. Comparing these spectra with reference samples confirms reproducibility and structural integrity of **PTA** samples, which serves as a critical step in validating the methodology before scaling up.

In the FTIR spectra of **PTA** samples synthesized at lower temperatures (Fig. S2), the absorption band at 1744  $\text{cm}^{-1}$  is significantly less intense compared to that observed in the FTIR spectrum of **PTA 1**, which was synthesized at a temperature of



Fig. 3 FTIR spectra of the **PTA** samples involved in the scaling process.



160 °C. This observation indicates that polymers synthesised at higher thermal conditions lead to the development of the polymer structure for **PTA**. Additionally, the other absorption bands present in the FTIR spectra of **PTA 3** and **PTA 4** are much broader than those from the FTIR spectrum of **PTA 1**. These observations indicate H-bridging by OH-groups, meaning that a considerable amount of monomer was not polymerised for these two samples synthesised at a lower temperature. This finding emphasises the critical role of synthesis temperature in influencing the spectral characteristics of **PTA** samples.

### Thermogravimetric analyses of poly(tartaric acid)

Thermogravimetric analysis (TGA) was employed to investigate the thermal stability and decomposition behaviour of the up-scaled **PTA** samples. For **PTA**, TGA curves offer valuable insights (Fig. 4) into its weight loss patterns during thermal degradation. Typically, the TGA curve of **PTA** exhibits distinct weight loss steps, corresponding to the evaporation of water, decarboxylation reactions, decomposition of COOH side groups, and the breakdown of the polymer backbone. When scaling up the synthesis of polytartaric acid, reaction parameters such as temperature control, mixing efficiency, and reaction time may vary, resulting in slight differences in the TGA curves. The weight loss profile for the non-upscaled sample **PTA 1** demonstrates a gradual mass loss of 10% up to 180 °C. This loss is primarily attributed to the elimination of both intra- and intermolecular water, as well as the release of CO<sub>2</sub>. Additionally, some of this mass loss may be due to the adsorbed water present in the polymeric sample. In contrast, the upscale samples exhibit better thermal stability. For example, **PTA 9**, synthesized from 500 g, remains stable up to 170 °C, while **PTA 8**, synthesized from 50 g, maintains stability up to 185 °C. Probably, the number of carboxy and OH groups that give rise to decarboxylation and the elimination of water is reduced. Beyond 180 °C, the trend in mass loss becomes consistent across all three samples. We also observe that the

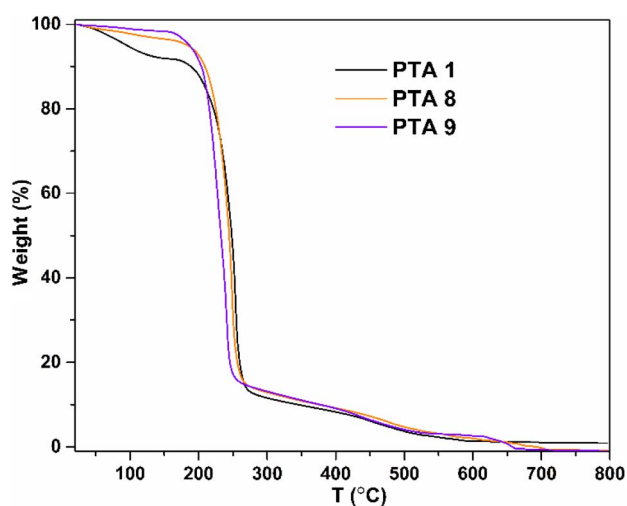


Fig. 4 TGA curve of spectra of the **PTA** samples involved in the scaling process.

decomposition steps are narrow, indicating that we obtained a limited range of polymer molecular structures, which has resulted in tighter thermal degradation profiles for all samples.

In conclusion, after analysing the polymer TGA curves, the scale-up polymerisation reaction of tartaric acid does not reduce the polymer thermal stability.

### Thermal conductivity analysis of up-scaled **PTA**

This study also aimed to explore the effects of the upscaling polymerisation reaction on the thermal conductivity and diffusivity of **PTA**. To achieve this, we employed the transient plane source (TPS) method, which is particularly advantageous as it enables the extraction of essential thermophysical parameters, such as thermal conductivity ( $\lambda$ ), thermal diffusivity ( $\alpha$ ), and specific heat, from a single transient recording. Even if all these parameters are essential in this study, we focused solely on the  $\lambda$  of the **PTA**. It is well known that the presence of structural defects within polymers can lead to phonon scattering, which significantly diminishes  $\lambda$ . The morphology of the polymer has a considerable impact on its  $\lambda$ . When amorphous domains dominate, vibrational modes become localized, lowering  $\lambda$ .

In Fig. 5, it is apparent that the  $\lambda$  of the up-scaled samples, particularly **PTA 8** ( $\lambda = 0.23 \text{ W mK}^{-1}$ ) and **PTA 9** ( $\lambda = 0.25 \text{ W mK}^{-1}$ ), is marginally higher than that of the small-scale samples. Furthermore, it is important to highlight that the samples synthesized at lower temperatures, specifically **PTA 3** (150 °C) and **PTA 4** (140 °C), exhibit lower thermal conductivity ( $\lambda = 0.16 \text{ W mK}^{-1}$  and  $\lambda = 0.15 \text{ W mK}^{-1}$ , respectively) compared to the **PTA** samples synthesized at 160 °C. This decrease in thermal conductivity indicates again that a portion of the tartaric acid remains unreacted when **PTA** is prepared at a lower temperature.

## Experimental

### Materials

L-Tartaric acid was purchased from Merck and used without further purification. Bromothymol blue, sodium hydroxide (NaOH) and ethanol were purchased from Alfa Aesar and also used without additional purification.



Fig. 5 Thermal conductivity of **PTA** samples involved in the upscaling reaction.



## Polytartaric acid

A method similar to the one previously described<sup>31</sup> was employed to synthesise all **PTA** samples, which are the subject of this paper. **TA** was ground into a fine powder using a mortar and transferred into a wide beaker. The beaker was placed in an oven and heated at various temperatures for 6 hours. Near the end of the reaction, the mixture in the beaker began to rise, forming bubbles. After cooling to room temperature, a solid was obtained. Table 1 outlines all the experiments conducted to synthesise different samples, spanning the transition from small-scale to large-scale synthesis of **PTA**.

## Methods of quality control

During the titration of the carboxy group, bromothymol blue was employed as an indicator. This pH-sensitive dye exhibits a colour change from yellow at a pH of 6.0 to blue at a pH of 7.6, rendering it particularly suitable for titrations involving weak acids. To initiate the titration process, 0.1 mL of bromothymol blue was mixed with ethanol. Subsequently, 0.2 g of the **PTA** sample was dissolved in 30 mL of water to create a suspension, to which eight drops of bromothymol blue were added for each sample solution. Using a burette, the solution was titrated with 0.1 M NaOH while maintaining continuous stirring. Throughout the titration, a colour transition from yellow to green was observed, indicating that the pH was approaching neutrality. The process was carried out until the solution developed a blue hue, signifying the equivalence point. Fourier transform infrared (FTIR) spectra were recorded using a JASCO FTIR 4600A spectrophotometer with an ATR-PRO-ONE accessory. Solid-state <sup>13</sup>C NMR (<sup>13</sup>C ss-NMR) spectra were recorded at a 125.73 MHz Larmor frequency using a Bruker Avance III 500 MHz wide-bore NMR spectrometer operating at room temperature. The sample was packed in 4 mm zirconia rotors and analysed with a 4 mm double resonance (1H/X) MAS probe. Peak assignments were performed by simulation using ACD/Labs 12.00 software. Standard RAMP CPMAS spectra were acquired at a spinning frequency of 14 kHz, a contact time of 2 ms, and with proton decoupling under TPPM. The acquisition parameters were optimised to the following values of relaxation delay and number of transients: 30 seconds and 2000 transients, respectively. The recorded spectra are calibrated relative to the CH<sub>3</sub> line in TMS (tetramethylsilane) through an indirect procedure, which utilizes L-glycine as an external standard (CO of glycine at 176.5 ppm). Thermogravimetry measurements were performed in air using TA Instruments SDT Q600 equipment, with a temperature range of 30 to 800 °C and a heating rate of 10 °C min<sup>-1</sup>. The thermal conductivity was measured using a Hot Disk TPS 2500 S (Hot Disk AB, Kagaku, Sweden) apparatus with a 5464F1 sensor, employing the transient plane source (TPS) method. The equipment has included determining the diffusivity and specific heat of materials. The method's principle involves applying a short heat pulse of predetermined duration to the sample, which is initially kept at thermal equilibrium. This is achieved using a TPS sensor with dual functions: serving as both a constant heat source and a temperature sensor, placed between two identical samples. The transient

temperature response of the samples is recorded and is further used to estimate the thermal conductivity. To get results with excellent accuracy, the samples were prepared in the form of identical pellets with a radius of 5 cm and a thickness of about 4 mm to ensure that we could use a TPS sensor with a diameter of 2 mm so that the heat generated by the spiral area does not diffuse to the sample outside boundary within a predefined period of measurement time.

## Conclusions

The polymerisation of **TA** to **PTA** uses sustainable natural starting material, omits solvents and catalysts and produces just water and carbon dioxide as by-products, thus contributing to the concept of “green chemistry”. The product possesses functional groups useful for functionalisation, such as carboxy and hydroxy and offers interesting practical applications. So far, **PTA** has only been synthesised on a small scale. In order to provide larger quantities as needed for such applications, the polymerization was successfully upscaled to a 500 g batch. A useful apparatus was constructed, and the properties of the different batches depending on batch size and temperature were investigated using solid-state NMR spectroscopy and IR spectroscopy. The results confirmed that the properties of the 500 g batch were identical to those of smaller-scale syntheses. Furthermore, the thermal properties of **PTA**, as determined by TGA and thermal conductivity, underscore the success of the upscaling process. These findings validate the robustness of the polymerization methodology, demonstrating its scalability while preserving chemical integrity. In conclusion, the synthesised **PTA**, being a polycarboxylic acid, presents promising opportunities across diverse industries, thereby reinforcing the relevance of sustainable polymer chemistry in contemporary material science.

## Author contributions

Iulia Rigo: writing – review & editing, methodology, data curation, formal analysis. Alexander Bunge: formal analysis, methodology. Lucian-Cristian Pop: data curation, writing – review & editing, supervision. Natalia Terenti: review & editing, resources, methodology, investigation, funding acquisition, conceptualization. Alexandrina Nan: writing – review & editing, writing – original draft, visualisation, formal analysis, data curation, project administration, supervision.

## Conflicts of interest

There are no conflicts to declare.

## Data availability

All data have been provided in the main article and the SI. Supplementary information: Fig. S1: FTIR spectra of **PTA** samples prepared for scaling up polymerisation reaction and Fig. S2: FTIR spectra of **PTA** samples obtained at different temperatures. See DOI: <https://doi.org/10.1039/d5su00667h>.



## Acknowledgements

The authors gratefully acknowledge the support of the Ministry of Education and Research, UEFISCDI, project number PN-IV-P2-2.1-TE-2023-0129, contract no. 94TE/03.01.2025. The authors would like to acknowledge Dr Monica Dan and Dr Xenia Filip from the National Institute for Research and Development of Isotopic and Molecular Technologies in Cluj-Napoca for conducting the TGA measurements and solid-state C-NMR experiments.

## Notes and references

- 1 R. Mohan, V. Chakravarthi, T. V. Nagaraju, S. Avudaiappan, T. F. Awolusi, A. Roco-Videla, M. Azab and P. Kozlov, *Case Stud. Constr. Mater.*, 2023, **18**, e02200, DOI: [10.1016/j.cscm.2023.e02200](https://doi.org/10.1016/j.cscm.2023.e02200).
- 2 X. Wang, A. L. Chin, J. Zhou, H. Wang and R. Tong, *J. Am. Chem. Soc.*, 2021, **143**, 16813–16823, DOI: [10.1021/jacs.1c08802](https://doi.org/10.1021/jacs.1c08802).
- 3 C. M. Rochman, M. A. Browne, B. S. Halpern, B. T. Hentschel, E. Hoh, H. K. Karapanagioti, L. M. Rios-Mendoza, H. Takada, S. The and R. C. Thompson, *Nature*, 2013, **494**, 169–171, DOI: [10.1038/494169a](https://doi.org/10.1038/494169a).
- 4 Y. Zhu, C. Romain and C. K. Williams, *Nature*, 2016, **540**, 354–362, DOI: [10.1038/nature21001](https://doi.org/10.1038/nature21001).
- 5 M. Hong and E. Y. X. Chen, *Green Chem.*, 2017, **19**, 3692–3706, DOI: [10.1039/C7GC01496A](https://doi.org/10.1039/C7GC01496A).
- 6 R. Kumar, A. Verma, A. Shome, R. Sinha, S. Sinha, P. K. Jha, R. Kumar, P. Kumar, S. Das, P. Sharma and P. V. V. Prasad, *Sustainability*, 2021, **13**, 9963, DOI: [10.3390/su13179963](https://doi.org/10.3390/su13179963).
- 7 N. Singh and T. R. Walker, *npj Mater. Sustainability*, 2024, **2**, 17, DOI: [10.1038/s44296-024-00024-w](https://doi.org/10.1038/s44296-024-00024-w).
- 8 M. A. Hillmyer and W. B. Tolman, *Acc. Chem. Res.*, 2014, **47**, 2390–2396, DOI: [10.1021/ar500121d](https://doi.org/10.1021/ar500121d).
- 9 G. W. Coates and Y. D. Y. L. Getzler, *Nat. Rev. Mater.*, 2020, **5**, 501–516, DOI: [10.1038/s41578-020-0190-4](https://doi.org/10.1038/s41578-020-0190-4).
- 10 O. Dechy-Cabaret, B. Martin-Vaca and D. Bourissou, *Chem. Rev.*, 2004, **104**, 6147–6176, DOI: [10.1021/cr040002s](https://doi.org/10.1021/cr040002s).
- 11 J. B. Zhu, E. M. Watson, J. Tang and E. Y. X. Chen, *Science*, 2018, **360**, 398–403, DOI: [10.1126/science.aar5](https://doi.org/10.1126/science.aar5).
- 12 C. M. Thomas, *Chem. Soc. Rev.*, 2010, **39**, 165–173, DOI: [10.1039/B810065A](https://doi.org/10.1039/B810065A).
- 13 Q. Feng, L. Yang, Y. Zhong, D. Guo, G. Liu, L. Xie, W. Huang and R. Tong, *Nat. Commun.*, 2018, **9**, 1559, DOI: [10.1038/s41467-018-03879-5](https://doi.org/10.1038/s41467-018-03879-5).
- 14 Z. Song, Z. Tan and J. Cheng, *Macromolecules*, 2019, **52**, 8521–8539, DOI: [10.1021/acs.macromol.9b01450](https://doi.org/10.1021/acs.macromol.9b01450).
- 15 J. Chen, Y. Dong, C. Xiao, Y. Tao and X. Wang, *Macromolecules*, 2021, **54**, 2226–2231, DOI: [10.1021/acs.macromol.0c02689](https://doi.org/10.1021/acs.macromol.0c02689).
- 16 M. Byrne, D. Victory, A. Hibbitts, M. Lanigan, A. Heise and S. A. Cryan, *Biomater. Sci.*, 2013, **1**, 1223–1234, DOI: [10.1039/C3BM60123D](https://doi.org/10.1039/C3BM60123D).
- 17 J. Lian, J. Chen, S. Luan, W. Liu, B. Zong, Y. Tao and X. Wang, *ACS Macro Lett.*, 2022, **11**, 46–52, DOI: [10.1021/acsmacrolett.1c00658](https://doi.org/10.1021/acsmacrolett.1c00658).
- 18 M. Zheng, M. Pan, W. Zhang, H. Lin, S. Wu, C. Lu, S. Tang, D. Liu and J. Cai, *Bioact. Mater.*, 2021, **6**, 1878–1909, DOI: [10.1016/j.bioactmat.2020.12.001](https://doi.org/10.1016/j.bioactmat.2020.12.001).
- 19 T. Leigh and P. Fernandez-Trillo, *Nat. Rev. Chem.*, 2020, **4**, 291–310, DOI: [10.1038/s41570-020-0180-5](https://doi.org/10.1038/s41570-020-0180-5).
- 20 J. Schymura, M. Held and P. Georgopoulos, *Macromol. Chem. Phys.*, 2023, **224**, 2300119, DOI: [10.1002/macp.202300119](https://doi.org/10.1002/macp.202300119).
- 21 V. Garg, A. McCaslin, M. J. Forrester, B. W. Kuehl, S. Raman, D. Dileep and E. W. Cochran, *J. Chem. Eng.*, 2024, **499**, 155693, DOI: [10.1016/j.ccej.2024.155693](https://doi.org/10.1016/j.ccej.2024.155693).
- 22 W. Lv, M. Li and Y. Tao, *Chin. J. Chem.*, 2023, **41**, 2488–2492, DOI: [10.1002/cjoc.202300187](https://doi.org/10.1002/cjoc.202300187).
- 23 R. Mil-Martinez, A. Gomez-Lopez, J. P. Escandon, E. M. Jimenez, L. Martinez-Suastegui and R. O. Vargas, *Processes*, 2024, **12**, 1624, DOI: [10.3390/pr12081624](https://doi.org/10.3390/pr12081624).
- 24 L. I. Jacob and W. Pauer, *Polymers*, 2022, **14**, 1574, DOI: [10.3390/polym14081574](https://doi.org/10.3390/polym14081574).
- 25 A. R. S. Teixeira, G. Willig, J. Couvreur, A. L. Flourat, A. A. M. Peru, P. Ferchaud, H. Ducatele and F. Allais, *React. Chem. Eng.*, 2017, **2**, 406, DOI: [10.1039/c7re00017k](https://doi.org/10.1039/c7re00017k).
- 26 A. G. Fisch, *React. Chem. Eng.*, 2023, **8**, 2924, DOI: [10.1039/d3re00349c](https://doi.org/10.1039/d3re00349c).
- 27 G. Winzenburg, C. Schmidt, S. Fuchs and T. Kissel, *Adv. Drug Deliv. Rev.*, 2004, **56**, 1453–1466, DOI: [10.1016/j.addr.2004.02.008](https://doi.org/10.1016/j.addr.2004.02.008).
- 28 M. Okada, *Prog. Polym. Sci.*, 2002, **27**, 87–133, DOI: [10.1016/S0079-6700\(01\)00039-9](https://doi.org/10.1016/S0079-6700(01)00039-9).
- 29 Y. Tokiwa and B. P. Calabia, *J. Polym. Environ.*, 2007, **15**, 259–267, DOI: [10.1007/s10924-007-0066-3](https://doi.org/10.1007/s10924-007-0066-3).
- 30 S. Dhamaniya and J. Jacob, *Polymer*, 2010, **51**, 5392–5399, DOI: [10.1016/j.polymer.2010.09.034](https://doi.org/10.1016/j.polymer.2010.09.034).
- 31 J. J. Bou, A. Rodriguez-Galan and S. Muñoz-Guerra, *Macromolecular*, 1993, **26**, 5664–5670, DOI: [10.1021/ma00073a020](https://doi.org/10.1021/ma00073a020).
- 32 I. Villuendas, J. I. Iribarren and S. Muñoz-Guerra, *Macromolecular*, 1999, **32**, 8015–8023, DOI: [10.1021/ma991050v](https://doi.org/10.1021/ma991050v).
- 33 C. Regano, A. M. de Ilarduya, J. I. Iribarren and S. Muñoz-Guerra, *J. Polym. Sci., Part A: Polym. Chem.*, 2000, **38**, 2687–2696, DOI: [10.1002/1099-0518\(20000801\)38:15<2687::AID-POLA80>3.0.CO;2-Q](https://doi.org/10.1002/1099-0518(20000801)38:15<2687::AID-POLA80>3.0.CO;2-Q).
- 34 Y. Shibata and A. Takasu, *J. Polym. Sci., Part A: Polym. Chem.*, 2009, **47**(21), 5747–5759, DOI: [10.1002/pola.23619](https://doi.org/10.1002/pola.23619).
- 35 Z. Wu, Y. Huang, C. Zhang, D. Zhu, Z. Bian, M. Ding, L. Gao and Z. Yang, *J. Appl. Polym. Sci.*, 2010, **117**, 3558–3567, DOI: [10.1002/app.32264](https://doi.org/10.1002/app.32264).
- 36 S. Dhamaniya and J. Jacob, *Polymer*, 2010, **51**, 5392–5399, DOI: [10.1016/j.polymer.2010.09.034](https://doi.org/10.1016/j.polymer.2010.09.034).
- 37 S. Dhamaniya, D. Das, B. K. Satapathy and J. Jacob, *Polymer*, 2012, **53**(21), 4662–4671, DOI: [10.1016/j.polymer.2012.08.025](https://doi.org/10.1016/j.polymer.2012.08.025).
- 38 S. Dhamaniya and J. Jacob, *Polym. Bull.*, 2012, **68**(5), 1287–1304, DOI: [10.1007/s00289-011-0606-9](https://doi.org/10.1007/s00289-011-0606-9).
- 39 C. Japu, A. M. de Ilarduya, A. Alla and S. Muñoz-Guerra, *Polymer*, 2014, **55**, 2294–2304, DOI: [10.1016/j.polymer.2014.03.018](https://doi.org/10.1016/j.polymer.2014.03.018).



- 40 S. Dhamaniya, H. S. Jaggi, M. Nimiya, S. Sharma, B. K. Satapathya and J. Jacob, *Polym. Int.*, 2014, **63**, 680–688, DOI: [10.1002/pi.4569](https://doi.org/10.1002/pi.4569).
- 41 K. Zawada, A. Plichta, D. Jańczewski, H. Hajmowicz, Z. Florjańczyk, M. Stępień, A. Sobiecka and L. Synoradzki, *ACS Sustainable Chem. Eng.*, 2017, **5**, 5999–6007, DOI: [10.1021/acssuschemeng.7b00814](https://doi.org/10.1021/acssuschemeng.7b00814).
- 42 E. Zakharova, A. M. de Ilarduya and S. Leon, Muñoz-Guerra, *React. Funct. Polym.*, 2018, **126**, 52–62, DOI: [10.1016/j.reactfunctpolym.2018.03.007](https://doi.org/10.1016/j.reactfunctpolym.2018.03.007).
- 43 R. Imamura, K. Oto, K. Kataoka and A. Takasu, *ACS Omega*, 2023, **8**(26), 23358–23364, DOI: [10.1021/acsomega.2c07627](https://doi.org/10.1021/acsomega.2c07627).
- 44 A. Nan, X. Filip, M. Dan and O. Marincas, *J. Clean. Prod.*, 2019, **210**, 687–696, DOI: [10.1016/j.jclepro.2018.11.069](https://doi.org/10.1016/j.jclepro.2018.11.069).
- 45 A. Enumo Jr, I. P. Gross, R. H. Saatkamp, A. T. N. Pires and A. L. Parize, *Polym. Test.*, 2020, **88**, 106552, DOI: [10.1016/j.polymertesting.2020.106552](https://doi.org/10.1016/j.polymertesting.2020.106552).

